International Journal Of Advanced Communication Technology (IJACT)
Volume 4, 2024 [19-28]

A Comparative Study of Binary and Fibonacci Decomposition Watermarking for Medical Images

Norsabihah Adnan[1] and Nur Hafizah Ghazali[2*]

[1]Faculty of Electronic Engineering & Technology, Universiti Malaysia Perlis (UniMAP), 02600 Arau, Perlis, Malaysia
[2]Centre of Excellence for Advanced Computing (AdvComp), Universiti Malaysia Perlis (UniMAP), 02600 Arau, Perlis, Malaysia

ABSTRACT

This study addresses the critical challenge of embedding additional information into medical images, specifically focusing on the trade-off between watermark capacity and visual quality. The importance of this challenge lies in maintaining the diagnostic value of medical images while securely embedding auxiliary data such as patient identifiers or copyright information. The study conducts a comparative analysis of two watermarking schemes: binary decomposition and Fibonacci decomposition. The binary and Fibonacci decompositions were specifically applied by utilizing modified binary watermarks and leveraging the specific domain properties of the host medical images to minimize disruptions during the embedding process. The evaluation was performed on a dataset of brain magnetic resonance imaging (MRI) images. The watermark capacity was varied to assess its impact on visual quality, which was quantified using Peak Signal-to-Noise Ratio (PSNR). The results demonstrated that the Fibonacci decomposition method achieved a higher watermark capacity of up to 3.5 bpp while maintaining high visual quality, with an average PSNR value of 76.5 dB. These results indicate that the Fibonacci decomposition approach offers significant advantages in achieving a balance between high capacity and minimal image distortion, making it a promising solution for medical image watermarking applications.

Keywords: Fibonacci decomposition, medical image watermarking, visual quality, watermark capacity

1. INTRODUCTION

The healthcare industry has experienced significant transformation driven by advancements in technology, revolutionizing various elements of patient care, from diagnosis and treatment strategies to remote monitoring and data management. In this context, medical imaging plays a crucial function, delivering invaluable insights anatomy, physiology, and disease progression. Modalities such as X-ray, CT scans, and MRIs provide detailed visual representations of internal structures, facilitating precise diagnoses and decisions regarding treatment.

The widespread utilization of digital medical images, however, poses a significant challenge in terms of embedding capacity. In contrast to conventional film-based imaging, digital images exhibit limited storage capabilities. This aspect becomes crucial when considering the need to incorporate additional data within the image itself [5], [8], [10]. Watermarking or data-hiding techniques offer a potential solution, enabling the secure integration of auxiliary data such as patient identifiers, timestamps, or copyright information [1], [7]. However, these techniques face a constant trade-off between embedding capacity and the visual quality of the watermarked image. Overly aggressive embedding can introduce distortions that compromise the diagnostic value of the image.

*hafizahghazali@unimap.edu.my

The field of medical image watermarking has seen a surge in research activity, driven by the need to embed additional information within the images themselves. This information can include patient identifiers, timestamps, or copyright data. Studies like those by [3], [5] and [8] exemplify this focus on increasing the embedding capacity. However, a key limitation remains. Traditional techniques primarily rely on representing the watermark information using binary data or primary colour components. This approach suffers from two main drawbacks. First, binary data inherently offers a limited capacity for encoding complex information. Second, current techniques may not fully exploit the significant redundancy present within medical images, hindering their ability to efficiently embed the watermark.

While [3], [5] and [9] focus on specific methods to achieve high capacity, other works explore alternative approaches. Sabbane and Tairi [6] proposed a watermarking technique based on polynomial decomposition, which may offer advantages in terms of robustness. Similarly, Bastani and Ahouz [2] investigated the use of Tchebichef moments for high-capacity and secure watermarking. It's worth noting that research by [4] explored a hybrid scheme combining the Hamming code, Least Significant Bit (LSB), and Optimal Pixel Adjustment Process (OPAP) for data hiding in medical images. This approach aimed to achieve a balance between embedding capacity, security, and imperceptibility. These studies highlight the ongoing exploration of diverse techniques to overcome the limitations of traditional binary embedding.

Furthermore, reversible watermarking techniques, like those proposed by [8] and [11], offer an attractive solution for medical images. These techniques allow for the original image to be perfectly recovered after watermark extraction. However, even in these advancements, the core limitation of information density in the watermark itself remains.

This comparative study investigates two watermarking methods for medical images: binary and Fibonacci decomposition. While binary data is the most common approach, Fibonacci decomposition offers a more intricate and information-rich representation for the watermark. This potentially enables a significant improvement in embedding capacity while maintaining the critical visual quality required for accurate medical diagnosis.

2. PROPOSED TECHNIQUE

The proposed technique introduces a novel data hiding method for medical image watermarking. This method leverages Fibonacci sequence decomposition during the preprocessing stage. The decomposition aims to generate additional bit planes for watermark embedding while minimizing distortion to the original image.

Traditional binary representation suffers from two main limitations, as discussed earlier. First, its reliance on just 0s and 1s limits information density. Second, it may not fully exploit the significant redundancy present within medical images for watermark embedding.

Fibonacci decomposition offers a potential solution by providing a more intricate and information-rich representation compared to binary data. This approach can lead to two key improvements. First, the additional bits generated through decomposition allow for embedding a larger amount of watermark information without compromising image quality. Second, by manipulating bits in less significant planes, the impact on visual quality is minimized compared to modifying binary data directly.

The proposed technique decomposes the 16-bit host image into 22-bit planes using Fibonacci numbers. This decomposition aims to generate additional planes for watermark embedding while minimizing distortion to the original image.

A crucial factor is the number of bit planes. This is determined by the sum of Fibonacci sequence values needed to exceed the maximum value (65535) representable by a 16-bit binary number. Equation (1) calculates this sum.

$$P = f(n+2) - f(2) \tag{1}$$

Since a 16-bit binary number can represent a maximum value of 65535, the calculation essentially finds the total number of Fibonacci sequence values that add up to or exceed this value. This calculation reveals that 22 Fibonacci numbers, starting from 1 and culminating in 28657, are required to achieve this sum. Consequently, 22-bit planes are necessary to represent the host image in the Fibonacci domain.

Figure 1 provides the pseudo-code for this decomposition process. The algorithm iteratively calculates Fibonacci numbers and utilizes them to extract bit planes from the original 16-bit host image.

```
Input: A 16 bits of host image
Output: A 22-bit planes of host image

Begin:
        read host image i
        initialize bit plane BP, Fibonacci number fibnum
        set counter x = 22, fibnum(0) = 1, fibnum(1) = 1
        for x > 0
                // calculate the x-th Fibonacci number
                fib(x) = fibnum(x-1) + fibnum(x-2)

                //calculate the set of x-th bit
                BP(x) = floor(i/ fibnum(x))

                // set new value to i
                i = i – (BP(x) * fibnum(x))

                //decrease the value of counter x
                x = x - 1
        end for
end
```

Figure 1. Pseudo-code of the Fibonacci decomposition process for a 16-bit host image into 22-bit planes.

Following this decomposition process, the host image is transformed into 22 individual bit planes. These bit planes represent the image data in the Fibonacci domain and serve as the foundation for the subsequent watermark embedding stage.

Compared to binary representation, Fibonacci decomposition offers several advantages. With 22 bits, the Fibonacci representation allows for a wider range of values compared to the binary limitation for the same number of bits (Table 1). Modifications to lower-order bit planes in the Fibonacci domain have a lesser visual impact compared to binary representation due to their role in representing finer image details (Table 2).

Table 1 Comparison of value representation between binary and Fibonacci sequences

Bit plane	1	2	3	4	5	6	7	8
Binary	2	4	8	16	32	64	128	256
Fibonacci	1	2	3	5	8	13	21	34

Bit plane	9	10	11	12	13	14	15	16
Binary	512	1024	2048	4096	8192	16384	32768	65536
Fibonacci	55	89	144	233	377	610	987	1597

Table 2 Maximum allowed bit error for each bit plane after watermark embedding

Bit plane	1	2	3	4	5	6	7	8
Binary	+1	+2	+4	+8	+16	+32	+64	+128
Fibonacci	+1	+2	+3	+5	+8	+13	+21	+34

Bit plane	9	10	11	12	13	14	15	16
Binary	+256	+512	+1024	+2048	+4096	+8192	+16384	+32768
Fibonacci	+55	+89	+144	+233	+377	+610	+987	+1597

Following decomposition, a verification process based on Zeckendorf's theorem (Section 2.1) ensures that each pixel value has a unique Fibonacci representation. This step guarantees the accuracy and efficiency of the embedding process. The subsequent section will delve into Zeckendorf's theorem and its application for verification in this proposed technique.

2.1 Zeckendorf's Theorem

The proposed Fibonacci decomposition technique offers a significant advantage: the ability to represent each pixel value uniquely. This is crucial for ensuring accurate watermark embedding and retrieval. However, a potential issue arises - a single decimal value can be represented by multiple Fibonacci sequences. This redundancy can lead to errors during the watermarking process. For instance, the number 76 can be expressed as a sum of Fibonacci numbers in two ways:

i. 55 + 21 (101000000_F)
ii. 55 + 13 + 8 (1001100000_F)

To address this redundancy and guarantee a unique representation for each pixel value, Zeckendorf's theorem is employed. This theorem states that every positive integer can be uniquely represented as a sum of distinct, non-consecutive Fibonacci numbers.

In simpler terms, Zeckendorf's theorem ensures that a number can only be expressed using a single combination of Fibonacci terms. These terms must be non-consecutive (i.e., no 1s appearing next to each other) and utilize the minimum number of Fibonacci values possible. This unique representation is symbolized as:

$$D = \sum_{i>2} b_i F_i \quad (2)$$

where $b_i \in \{0,1\}$ and $b_i b_{i+1} = 0$ for all $i > 2$. Following this rule, the unique Fibonacci representation for the number 76 becomes 101000000_F, signifying the absence of consecutive 1s and the use of the minimum Fibonacci terms possible.

By leveraging Zeckendorf's theorem, the proposed technique ensures a one-to-one mapping between pixel values and their Fibonacci representations. This uniqueness is vital for maintaining data integrity during the watermark embedding and retrieval processes.

2.2 Watermark Generation

This subsection discusses watermark generation within the proposed technique. To ensure successful embedding, the watermark needs to be adapted to the statistical properties of the host image. Here, the focus is on determining the dominant pixel value (black or white) within the host image.

2.2.1 Statistical Analysis of Host Image

Analysing the statistical properties of the host image is a critical step in the proposed technique for two key reasons. First, this information is used to modify the caption watermark. By understanding the dominant pixel value (black or white) within the image, the watermark can be adapted to ensure a more suitable embedding process. For instance, if black pixels are more prevalent, the watermark can be modified to contain mostly zeros to minimize disruption during embedding.

Second, the statistical analysis guides the selection of appropriate bit planes for watermark embedding. The distribution of black and white pixels across different bit planes (both binary and Fibonacci representations) helps determine which planes offer the optimal balance for successful watermark integration with minimal impact on the original image.

The proposed approach analyses the statistical properties of the last two-bit planes in both binary and Fibonacci domains. Tables 3 and 4 compare the binary decomposition for pixels with 0s (black) and 1s (white) values in the last two-bit planes. These tables reveal that for both planes, black pixels (0s) dominate, accounting for around 63% of the total pixels.

Table 3 Comparison of 0 and 1 pixel value representation in bit plane 1 (binary domain)

Brain MRI	Number of Pixels with 0 Value	Number of Pixels with 0 Value	0's Percentage	1's Percentage
MRI1	40997	24539	62.56	37.44
MRI2	41773	23736	63.74	36.26
MRI3	41452	24084	63.25	36.75
MRI4	41256	24280	62.95	37.05
MRI5	41431	24105	63.22	36.78

Table 4 Comparison of 0 and 1 pixel value representation in bit plane 2 (binary domain)

Brain MRI	Number of Pixels with 0 Value	Number of Pixels with 0 Value	0's Percentage	1's Percentage
MRI1	41116	24420	62.74	37.26
MRI2	41636	23900	63.53	36.47
MRI3	41572	23964	63.43	36.57
MRI4	41377	24159	63.14	36.86
MRI5	41253	24283	62.95	37.05

Similarly, Tables 5 and 6 compare the Fibonacci decomposition for 0s and 1s pixel values in the last two-bit planes. These tables demonstrate an even stronger dominance of black pixels in the Fibonacci domain. Here, the percentage of black pixels reaches 72% and 83% for bit planes 1 and 2, respectively.

Table 5 Comparison of 0 and 1 pixel value representation in bit plane 1 (Fibonacci domain)

Brain MRI	Number of Pixels with 0 Value	Number of Pixels with 0 Value	0's Percentage	1's Percentage
MRI1	46531	19005	71.00	29.00
MRI2	47123	18413	71.90	28.10
MRI3	47188	18348	72.00	28.00
MRI4	46929	18607	71.61	28.34
MRI5	46935	18601	71.62	28.38

Table 6 Comparison of 0 and 1 pixel value representation in bit plane 2 (Fibonacci domain)

Brain MRI	Number of Pixels with 0 Value	Number of Pixels with 0 Value	0's Percentage	1's Percentage
MRI1	53984	11552	82.37	17.63
MRI2	54235	11301	82.76	17.24
MRI3	54013	11523	82.42	17.58
MRI4	54221	11315	82.73	17.27
MRI5	54129	11344	82.69	17.13

Based on the comparisons, a significantly higher concentration of black pixels is observed in the Fibonacci representation compared to binary. To accommodate this characteristic, the caption watermark requires modification. This modification aims to maximize the number of zeros possible. This minimizes the impact of LSB insertion during the embedding process. Conversely, the number of ones in the watermark should be minimized. This prevents disruption of the dominant black pixels within the host image. In essence, this modification reduces the potential for errors that might arise during watermark embedding.

2.2.2 Watermark Modification

This section discusses the modification process applied to the caption watermark, which is initially patient data in text format. Table 7 compares the number of zeros and ones in the binary representation of uppercase and lowercase letters.

Table 7 Binary representation of lowercase and uppercase letters

Letter Case	Total Number of 0's	Total Number of 1's
Lowercase	96	112
Uppercase	122	86

Based on this comparison, it reveals that the binary representation of lowercase letters contains more ones (1s) compared to uppercase letters. The host image, in the Fibonacci domain, has a higher proportion of black pixels (represented by 0s). To minimize disruptions during watermark embedding, the watermark needs to have more zeros and fewer ones. Therefore, the modification focuses on the binary representation of lowercase letters because they inherently contain more ones, allowing for a more significant reduction in ones compared to uppercase letters. This reduction helps minimize the impact on the dominant black pixels in the host image, leading to a more robust watermark embedding process.

The modification involves removing the second and third bits from the original binary representation of lowercase letters. These bits are considered redundant for this purpose. The modified binary representation is shown in Table 8. This modification significantly increases the number of zeros in the watermark while reducing the number of ones.

Table 8 Modified binary representation of lowercase letters

Total Number of 0's	Total Number of 1's
148	60

The effect of watermark modification is then analyzed by examining the change in pixel value modification probability across bit planes (Tables 9 and 10). This probability is influenced by the number of zeros and ones in both the watermark and the host image. The significant decrease observed after modification indicates a lower risk of distortion in the final watermarked image.

Table 9 Probability change of 0s and 1s in bit planes 1 and 2 (Fibonacci domain)

Watermark	Bit Plane	Probability of Change	Probability of Stay
Original	1	0.5168	0.4832
	2	0.5250	0.4750
Modified	1	0.4069	0.5931
	2	0.3605	0.6395

The modified binary representations of lowercase letters are assembled to form a final, sequential stream of bits. This stream serves as the modified watermark ready for embedding into the host image.

3. RESULTS AND DISCUSSION

The effectiveness of the proposed watermarking technique was evaluated using a set of 10 brain MRI images. These images were obtained from the OsiriX-DICOM Viewer website, a resource known for providing datasets specifically for research and education. Each image adheres to the following specifications: grayscale DICOM format, 256 x 256 pixel resolution, and 16-bit depth.

Before embedding the watermark into the host images, it undergoes a modification process as discussed earlier. An example of the watermark used to evaluate the technique is depicted in Figure 2.

Patient Ref. No: AX8865098
Name of the doctor: Dr. Wu
Age: 48 years
Address: 22 Midland Ave.
Case History:
Date of admission: 18.05.2001
Results: T wave inversion
Diagnosis: Suspected MI

Figure 2. Example of watermark

This study investigates the relationship between embedding capacity and the visual quality of the watermarked images. To achieve this, different watermark sizes were embedded into the brain MRI images. The embedding capacity was systematically increased from 0.5 bits per pixel (bpp) to its maximum value, with each step incrementing by 0.5 bpp.

The visual quality of the watermarked images was assessed using the Peak Signal-to-Noise Ratio (PSNR). Generally, for 16-bit images, typical PSNR values considered acceptable range from 60 dB to 80 dB. The results of these experiments are tabulated in Table 10.

Table 10 PSNR Values of Watermarked Images Sized 256 × 256 for Different Embedding Capacities

Capacity (bpp)	Bit Planes Used	PSNR									
		MRI1	**MRI2**	**MRI3**	**MRI4**	**MRI5**	**MRI6**	**MRI7**	**MRI8**	**MRI9**	**MRI10**
0.5	1	101.37	101.33	101.34	101.32	101.36	101.35	101.39	101.34	101.35	101.35
1.0	2	98.19	98.16	98.18	98.14	98.17	98.17	98.22	98.15	98.18	98.17
1.5	3	91.87	91.81	91.82	91.79	91.78	91.78	91.91	91.81	91.82	91.80
2.0	3	88.53	88.46	88.48	88.48	88.45	88.43	88.56	88.45	88.50	88.47
2.5	5	83.68	83.57	83.63	83.55	83.61	83.52	83.72	83.55	83.66	83.59
3.0	5	79.94	79.85	79.90	79.81	79.90	79.80	80.03	79.80	79.93	79.82
3.5	6	76.64	76.48	76.56	76.44	76.51	76.43	76.78	76.43	76.62	76.49

As shown in Table 10, the proposed technique successfully embeds watermarks with a capacity of up to 3.5 bpp for host images sized 256 x 256 pixels. This embedding process utilizes six-bit planes derived from the host image decomposition. Employing a larger number of bit planes would introduce distortion in the watermarked image. For example, increasing the capacity to 3.6 bpp results in noticeable distortion, readily perceivable by the Human Visual System (HVS). This is primarily because using seven-bit planes becomes necessary, exceeding the optimal limit. Figure 3 presents a comparison between the original MRI1 image and its corresponding watermarked version with a distorted appearance due to a capacity of 3.6 bpp.

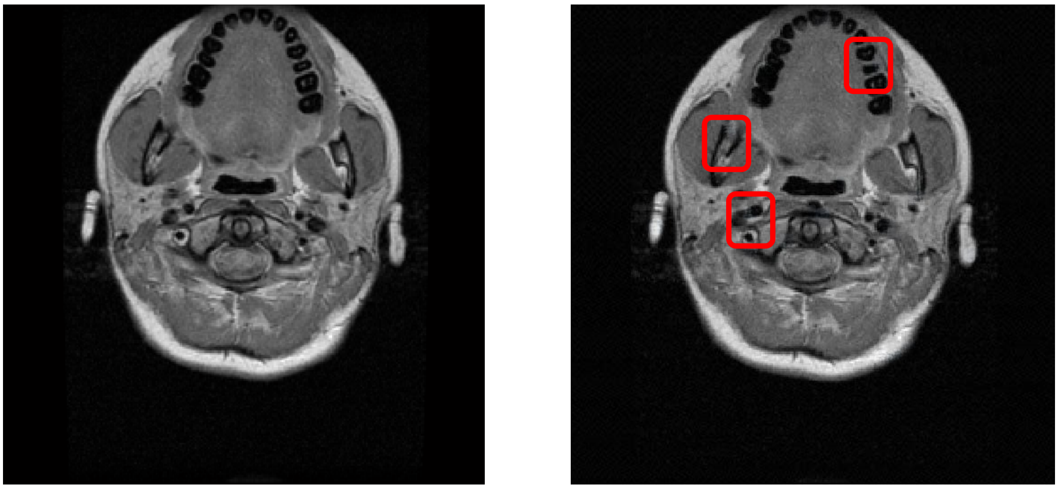

(a) (b)

Figure 3. (a) Original MRI1, (b) Watermarked MRI1 (3.6 bpp)

Despite the high watermark capacity (3.5 bpp), the visual quality of the watermarked images remains excellent. This is evidenced by the average PSNR value of 76.5370 dB, indicating minimal distortion introduced by the watermarking process. Individual PSNR values ranged from 76.4260 dB (MRI8) to 76.7769 dB (MRI7), demonstrating consistency across the test images.

4. CONCLUSION

This paper investigated a novel watermarking technique designed for embedding watermarks into brain MRI images. The primary focus was on achieving a balance between embedding sufficient information and preserving the visual quality of the watermarked images. The technique successfully hid watermarks in MRI images (up to 3.5 bpp) while maintaining high image quality (average PSNR of 76.5 dB). This suggests the technique is useful for protecting MRI images, such as adding copyright information or verifying image authenticity. Further investigation could explore the robustness of the technique against various attacks commonly encountered in image watermarking.

ACKNOWLEDGEMENTS

The authors acknowledge the financial support provided by the Ministry of Higher Education through the Fundamental Research Grant Scheme for Research Acculturation of Early Career Researchers (RACER) under a grant number of RACER/1/2019/ICT05/UNIMAP//1.

REFERENCES

[1] A. Al-Haj, H. Abdel-Nabi, "An efficient watermarking algorithm for medical images," Multimed Tools Appl, vol. 80, pp. 26021–26047, Jan 2021. doi.org/10.1007/s11042-021-10801-7.
[2] A. Bastani and F. Ahouz, "High Capacity and Secure Watermarking for Medical Images Using Tchebichef Moments," Radioengineering, vol. 29, no. 4, pp. 636-643, Sept. 2020. doi.org/10.13164/re.2020.0636.
[3] Ahmed Elhadad, A Ghareeb, Safia Abbas, "A blind and high-capacity data hiding of DICOM medical images based on fuzzification concepts," Alexandria Engineering Journal, vol. 60, pp. 2471-2482, Apr 2021, doi.org/10.1016/j.aej.2020.12.050.
[4] C. Kim, D. Shin, B. Kim, and C. Yang, "Secure medical images based on data hiding using a hybrid scheme with the Hamming code, LSB, and OPAP," Journal of Real-Time Image Processing, vol. 14, pp. 115-126, Feb 2017.
[5] E. Rayachoti, "A robust and high embedding capacity watermarking technique for telemedicine," The Imaging Science Journal, vol. 71, no. 6, pp. 537–548, Mar. 2023. doi:10.1080/13682199.2023.2186569.
[6] F. Sabbane and H. Tairi, "Medical image watermarking technique based on polynomial decomposition," Multimedia Tools and Applications, vol. 78, no. 23, pp. 34129–34155, Aug. 2019. doi:10.1007/s11042-019-08134-7.
[7] Khare P, Srivastava VK, "A Secured and Robust Medical Image Watermarking Approach for Protecting Integrity of Medical Images," Trans Emerging Tel Tech, vol. 32, no. 2, Feb 2021. doi.org/10.1002/ett.3918.
[8] L. Gao, Y. Zhang, and G. Li, "Reversible watermarking in medical images using sub-sample and multiple histogram modification," Journal of Information Technology Research, vol. 13, no. 4, pp. 75–90, Oct. 2020. doi:10.4018/jitr.2020100106.
[9] M. Nazari and M. Mehrabian, "A novel chaotic IWT-LSB Blind Watermarking approach with flexible capacity for secure transmission of authenticated medical images," Multimedia Tools and Applications, vol. 80, no. 7, pp. 10615–10655, Nov. 2020. doi:10.1007/s11042-020-10032-2.
[10] R. Geetha and S. Geetha, "Efficient high capacity technique to embed EPR information and to detect tampering in medical images," Journal of Medical Engineering & Technology, vol. 44, no. 2, pp. 55–68, Jan 2020. doi.org/10.1080/03091902.2020.1718223.

[11] X. Zhong and F. Y. Shih, “A high-capacity reversible watermarking scheme based on shape decomposition for medical images,” International Journal of Pattern Recognition and Artificial Intelligence, vol. 33, no. 01, p. 1950001, Oct. 2018. doi:10.1142/s0218001419500010.